

5-26-2021

## Effect of the Injector Viscous Damping on the Mass of Fuel injected During the Delay Period in Diesel Engines.

M. El-Kady

*Mechanical Power Department., Faculty of Engineering., El-Mansoura University., El-Mansoura., Egypt.,*  
mselkady@mum.mans.eun.eg

Salah El-Emam

*Associate Professor., Mechanical Power Engineering Department., Faculty of Engineering., El-Mansoura University., Mansoura., Egypt.,* sh\_lemam@mans.edu.eg

Follow this and additional works at: <https://mej.researchcommons.org/home>

---

### Recommended Citation

El-Kady, M. and El-Emam, Salah (2021) "Effect of the Injector Viscous Damping on the Mass of Fuel injected During the Delay Period in Diesel Engines.," *Mansoura Engineering Journal*: Vol. 14 : Iss. 2 , Article 17.

Available at: <https://doi.org/10.21608/bfemu.2021.172414>

This Original Study is brought to you for free and open access by Mansoura Engineering Journal. It has been accepted for inclusion in Mansoura Engineering Journal by an authorized editor of Mansoura Engineering Journal. For more information, please contact [mej@mans.edu.eg](mailto:mej@mans.edu.eg).

## EFFECT OF THE INJECTOR VISCOUS DAMPING ON THE MASS OF FUEL INJECTED DURING THE DELAY PERIOD IN DIESEL ENGINES.

تأثير تزويد البخاخ بمحمد هيدروليكي على كمية الوقود المحقونة خلال عطلة

الاشعال في محركات الديزل

By

M. S. El-KADY and S. H. El-Emam

Mechanical Power Department, Faculty of Engineering,  
Mansoura University, El-Mansoura, Egypt.

الخلاصة - يعتبر ضوضاء الاحتراق وانبعاشات غاز أول أكسيد النيتروجين من المشاكل الرئيسية في محركات الديزل وهي تحدث بسبب زيادة معدل التفاعل السريع في بداية الاحتراق نتيجة تراكم كمية الوقود المحقونة خلال عطلة الاشعال داخل الاسطوانة . ويهدف هذا البحث الى دراسة امكانية تزويد البخاخ بمحمد هيدروليكي مناسب وتأثير ذلك على كمية الوقود المحقونة خلال عطلة الاشعال . تم تطوير مبادئ نظري لمنظومة حقن الوقود في محركات الديزل وأمكن حساب الضغط في الأجزاء المختلفة لمنظومة حقن الوقود بتطبيق مبدأ الفروق المتناهية . وأيضاً حساب كل من حركة ابرة البخاخ وكمية الوقود المحقونة بتطبيق معادلات الحركة ونظرية الفوهتان على التوالي . كما تم تقدير نسبة تقليل كمية الوقود المحقونة خلال عطلة الاشعال باستخدام مخمدات هيدروليكية ذات معاملات اخمدان مختلفة . وللتحقق من نتائج الدراسة النظرية أجريت دراسة تجريبية تم خلالها تسجيل الضغط في خط توصيل الوقود من مضخة الحقن الى البخاخ في منظومة حقن الوقود لمحرك الديزل . وقد أظهرت نتائج المقارنة توافقاً مرضياً بين الضغط المسجل والقيم المحسوبة . ويستنتج من هذا البحث أنه من الممكن الحد من ضوضاء الاحتراق وانبعاشات غاز أول أكسيد النيتروجين في محركات الديزل بتقليل كمية الوقود المحقونة خلال عطلة الاشعال بنسب كافية وذلك عن طريق تزويد البخاخ بمحمد هيدروليكي مناسب .

**ABSTRACT**

The two major problems of automotive diesel engines, namely the combustion noise and high NO emissions can be reduced and become less serious by reducing the fuel mass injected during the delay period. The injector of the diesel fuel injection system is provided with a suitable viscous damping unit to increase the viscous friction force which resist the needle lift. In this paper, a general outline of the viscous damping unit is introduced and the considered fuel injection system is simulated numerically. The pressure in the different parts of the injection system is predicted using the theory of wave action where the finite difference principle has been incorporated. The needle valve motion is represented by the equation of motion and the rate of fuel injected is predicted using the theory of the two-orifices in series. The influence of the viscous damping on the injection process has been theoretically examined and the reduction percentage of the fuel mass injected during the delay period has been estimated for different values of damping coefficient.

An experimental study for the verification of the predicted results has been carried out. A satisfactory agreement between the predicted and the experimentally recorded results of pressure in the injection system has been observed. It is found that, providing an extra viscous damping to the injector of the injection system, keeps the rate of the fuel injected low at the start of the injection process, then the injection rate rises fast subsequently. As a result, a good reduction of the amount of the fuel injected during the expected delay period is obtained.

#### INTRODUCTION

Since the onset of the energy crises, there has been an upward trend to use the diesel engine for light duty vehicles and passenger cars in addition to its over increasing use in commercial automotive vehicles. This is mainly because the diesel engine is more efficient than its gasoline counterpart. However, the diesel engine operates at higher peak pressures and temperatures, higher rates of pressure rises and greater piston sideways forces, resulting in noisier operation and more NO emissions.

When ignition starts in a diesel engine, most of the fuel injected and intimately mixed with the air charge during the delay period burns almost instantaneously, releasing heat so quickly that the cylinder pressure rises rapidly. The sudden pressure rise generates a harsh combustion knock, and the high temperatures produced will allow nitrogen oxides to form in undesirable concentrations. The most effective reason for the increase of NO formation in diesel engines during combustion is the large mass of fuel that first enters the combustion chamber during the delay period.

Austen and Priede [1] also Russell and Haworth [2] showed that the combustion noise in diesel engines follows the rapid rate of pressure rise at the start of autoignition at the end of ignition delay. The rapid pressure rise causes high impulsive forces that creating the engine combustion noise. Kau et al. [3] found that the larger quantity of fuel presented when the combustion starts the higher percentage concentration of NO emission in the combustion products, because it attains the highest temperature and remains in a zone of high temperature longest. Therefore, both combustion noise and NO formation can be alleviated by reducing the mass of fuel injected during the initial part of the injection period.

In the jerk pump type of diesel injection systems the needle valve in the injector is under the influence of the pressure force due to the plunger movement, the spring force and the viscous friction force which is proportional to the needle valve velocity and always opposite to the valve movement. The viscous friction in most of diesel injection systems is very small and does not play any fundamental role in the injection process. But by providing the injection system with a suitable damping unit that the viscous friction force becomes considerable, then it is reasonable to expect that the rate of needle lift would become less steep which would probably reduce the fuel mass injected during the delay period. In this case the two major problems of automotive diesel engines, namely combustion noise and high NO

emissions, would become less serious.

The main objective of this work is to study the influence of the viscous friction force which resist the needle movement on the mass of fuel injected during the delay period in diesel engines. This could be achieved by using a viscous damper to be attached to the injector of the fuel injection system. A general outline of the viscous damper to has been introduced and its influence on the injection process has been examined theoretically by simulating the considered fuel injection system. This would indicate by how much (if at all) the mass of fuel injected during the delay period could be reduced with this method and the amount of damping needed to achieve this.

## 2. FUEL INJECTION SYSTEM SIMULATION

An early theoretical treatment of the injection process in diesel engines had been presented by Griffen and Rowe (4). It deals with an in-line jerk pump and takes into account the effect of pressure waves in the delivery pipe and the capacity effects of the volumes concentrated in the pump and nozzle system. Knight (5) introduced a model for viscous friction and cavitation in the delivery pipe of the fuel injection system. Becchi (6) used a model which comprised a detailed representation of the injector and the pump to describe the pressure wave action in the delivery pipe of the fuel injection system. Rosselli and Badgley (7) described a mathematical model for the analog simulation of the Cummins diesel injection system. A sophisticated simulation method has been reported by Wylie and co-workers (8-10). In this method the influence of factors such as wave propagation phenomena, pipe friction, cavitation, viscous friction at the needle valve and fuel leakage are taken into account. Yamaoka and Saito (11) and Yamaoka et al. (12) have reported a computer technique for evaluation of cavitation characteristics of certain phases of fuel injection in the diesel injection system. Also, Matsuoka et al. (13) studied the influence of the viscosity of fuel oil on the pressure wave damping, sound velocity and bulk modulus of the fuel oil in the delivery pipe of the diesel injection system. A flexible fuel injection simulation method has been recently reported by Dennis (14).

In the present study, it was aimed to study the effect of restraining the needle lift on the fuel mass injected during the delay period in diesel engines, the injection system simulation was only needed to provide a general assesment and not exact values. Great accuracy in the matching of the simulation results to the experimental data was not, therefore, of primary important. Most available simulation methods neglect the influence of viscous friction on the needle valve, while in this paper it is very important. A method was required that could easily be amended to deal with viscous friction as well as with the particular features of the injection pump fitted to the Perkins engine .

After considering these points it was decided to use the method of Griffen and Rowe (4) with a large number of modifications. Thus the treatment of the wave action in the pipe is identical, while that of the pump and injector had to be totally different.



The injection system assumed in the present study includes three major components: the fuel pump, the connecting fuel line and the fuel injector. The analytical model, which is programmed for a time variant simulation must include an accurate description of the geometrical and physical characters of the system as well as the equations that describe the dynamics of the fluid and the mechanical components. A total system analysis is necessary wherein ordinary differential equations describing each of fluid compressibility, delivery valve motion, and injector needle motion are handled numerically simultaneously with the numerical solution of the partial differential equations that describe the wave propagation phenomena in the fuel line.

### 2.1. The Rate of Injected Fuel

Figure 1 shows schematically the lower part of an injector nozzle of the diesel injection system. When the injection pressure  $P_1$  exceeds the opening pressure, the needle lifts and fuel enters the sac volume. The fuel pressure in the sac volume is an intermediate value between  $P_1$  and the cylinder pressure  $P_2$ . Assuming the same value  $C_d$  for the discharge coefficient of the needle seat and the injector holes, the following expression for the rate of discharge  $Q$  is obtained;

$$Q = \bar{A} C_d \sqrt{(2/\rho) (P_1 - P_2)} \quad (1)$$

where  $\rho$  is the fuel density,  $C_d$  is the needle discharge coefficient,  $P_1$ ,  $P_2$  are injection and cylinder pressure respectively and  $\bar{A}$  is the equivalent flow area for two orifices in series and is given by:

$$\frac{1}{\bar{A}^2} = \frac{1}{A_1^2} + \frac{1}{A_2^2} \quad (2)$$

where  $A_1$  is the flow area at the needle seat and  $A_2$  the total flow area through the injector holes

Equation (1) is used to calculate the rate of fuel injected when the injection pressure and the cylinder pressure are known.

Figure 2 shows a section through the lower part of the injection nozzle employed on the engine. If  $L$  is the needle lift, then  $A_1$  is equal to the area of the strip formed by the line segment  $ss'$ , when it is revolved  $360^\circ$  around the needle axis. Therefore;

$$A_1 = \pi L \sin \theta/2 (d - L \sin \theta/2 \cos \theta/2)$$

where  $L$  is the needle lift,  $d$  is the diameter of the sac volume and  $\theta$  is the cone angle of the needle.

The only unknown variable in Eq (1) is the discharge coefficient  $C_d$ . This depends on the nozzle configuration, the physical properties of the fuel, the needle lift and the pressure difference  $\Delta P = P_1 - P_2$ .

To determine the value of  $C_d$  in this particular injector,

measured values of the fuel injected per stroke is equated with the value given by integration of Eq. (1). With calculated value of  $C_d$  the rate of injection at every interval time was determined.

## 2.2 Needle Valve Motion

Applying Newton's second law to the needle valve shown in Fig. 2, the equation of motion can be written as follows:

$$M \ddot{x} = P A - K \delta - K x - \lambda f \dot{x}$$

where  $x$ ,  $\dot{x}$ ,  $\ddot{x}$  are the lift distance, velocity and acceleration of the needle respectively,  $\lambda$  is the sign of  $x$  (+ve for  $x > 0$  and -ve for  $x < 0$ ),  $K$  is the spring stiffness,  $M$  is the mass of the moving parts (needle valve and lift pick-up),  $f$  is the coefficient of viscous friction,  $\delta$  is the spring compression with closed valve and  $A$  is the maximum valve cross sectional area.

The equilibrium of forces when the valve just starts to open gives the following relationship;

$$K \delta = P_0 A_d$$

where  $A_d$  is the valve differential area. Therefore, the equation of motion of the needle valve can be written in the following form:

$$\ddot{x} + 2\lambda \nu \omega_n \dot{x} + \omega_n^2 x = \omega_n^2 x_0 \quad (3)$$

where  $\omega_n$  is the natural frequency =  $\sqrt{K/M}$ ,  
 $\nu$  is the damping coefficient =  $(f/2)/\sqrt{KM}$  and

$$x_0 = (PA - P_0 A_d)/K.$$

If the pressure varies linearly with time as;  $P = P(0) + Gt$  where  $P(0)$  is the pressure at  $t = 0$ ,  $G$  is the rate of pressure increase with time and taking the Laplace transformation for equation (3) the needle lift can be given by the following equation;

$$x = B_0 + B_1 e^{S_1 t} + B_2 e^{S_2 t} + B_3 t \quad (4)$$

$B_0, B_1, \dots, S_2$  are constants containing the values of the needle lift, needle velocity and injection pressure at  $t=0$  as well as the rate of pressure rise with the time,  $t$ .

$$\text{where } B_0 = y_0 - \frac{2\lambda \nu}{\omega_n} y,$$

$$B_1 = \frac{(2\lambda \nu \omega_n + S_1) [x(0) - B_0] + x(0) - B_3}{S_1 - S_2},$$

$$B_2 = \frac{(2\lambda \nu \omega_n + S_2) [x(0) - B_0] + x(0) - B_3}{S_2 - 1},$$

$$B_3 = y,$$

$$S_1 = -\omega_n (\lambda v + \sqrt{v^2 - 1}) ,$$

$$S_2 = -\omega_n (\lambda v - \sqrt{v^2 - 1}) ,$$

$$y_0 = \frac{[P(0) A - P_0 A_d]}{K} \quad \text{and}$$

$$y = A G/K$$

### 2.3 Theory of Wave Action in the Pipe

The treatment of the wave action in the pipe is identical to that mentioned by Griffen and Rowe (4). It can be summarized as follows:

#### Pump End

To solve the system it is necessary (in addition to all geometric, elastic and inertia characteristics of the various components involved in the phenomenon) to know the instantaneous velocity of the plunger  $v_p$  and the entity of the return pressure waves at the pump in the delivery duct  $P_r$  and the feeding duct  $P_f$ .

The continuity equation can be applied to the flow through the volume  $V_p$ . The rate of plunger displacement is equal to the rate of delivery of fuel into pipe plus the rate of compression of fuel in the volume  $V_p$  and the leakage rate  $Q_1$ . This can be written as follows:

$$A_p v_p = a v + \frac{v_p}{K} \cdot \frac{dP}{dt} + Q_1$$

Since  $v = (P_f - P_r) / \sqrt{\rho K}$  and  $P = P_f + P_r + P_k$ , the continuity equation becomes:

$$A_p v_p = \frac{a}{\sqrt{\rho K}} (P_f - P_r) + \frac{v_p}{K} \left[ \frac{dP_f}{dt} + \frac{dP_r}{dt} \right] + Q_1 \quad (5)$$

#### Nozzle End

The continuity equation can be applied to the volume  $V_n$  and yields that the rate of flow from the pipe into the nozzle will equal to the rate of compression of fuel in volume  $V_n$  due to valve movement. This can be written as follows:

$$\frac{a}{\sqrt{\rho K}} (P_f - P_r) = \frac{v_n}{K} \left[ \frac{dP_f}{dt} + \frac{dP_r}{dt} \right] + Q_{inj} + a_v \cdot \frac{dx}{dt} \quad (6)$$

where  $P_f$  and  $P_r$  are the instantaneous sum of the forward and backward

pressure waves respectively,  $v_n$  is the volume of fuel concentrated at nozzle end and  $a_v$  is the area of the valve exposed to pressure.

The finite difference method is used for equations (5) and (6) and the pressure at any point at the end of the time interval in the pipe line can be calculated from the known values at the beginning of the time interval. During the numerical solution the complete simulation for all components of the injection equipment including the cam profile, the pump and distributor timing was done with respect to the engine piston motion.

### 3. DAMPING SYSTEM

It is assumed that the damper can be fitted to the injector in the way shown in Fig. 3. The motion of the needle valve is transmitted to the damper through the damper rod as shown in Fig. 3. The damper acts as a braking system to decrease the velocity of the needle during its stroke.

An example of this damper is shown in Fig. 4.a. In this type of viscous dampers, the injected fuel can be used as a working fluid. The throttling of the fluid that flows from the cylinder to outside creates a pressure difference in the cylinder across the piston sides which causes the braking force  $F_b$  [15].

The flow rate through the orifice can be obtained as follows;

$$Q = C_d A_o \sqrt{2/\rho \cdot (P_b - P_1)}$$

Knowing from the continuity equation that  $Q = v_p \cdot A_p$  then the resulting force across the piston faces will be

$$F_b = A_p (P_b - P_1) = C_1 v_p^2$$

$$\text{where } C_1 = \frac{\rho}{2C_d^2} \cdot \frac{A_p^3}{A_o^2}$$

Another example for the viscous damper is shown in Fig. 4.b. In this type, the working fluid can be any kind of fluid according to the required braking force. As the injector needle opens the damper piston moves upward causing the fluid above the piston to move through the throttling pipe in the piston to the other side. According to the throttling pipe length and diameter a pressure difference across the piston sides in the cylinder will be formed. That will create the braking force.

For a laminar flow through the throttling pipe the pressure difference will take, due to Darcy's law, the following form;

$$P_b - P_1 = 32 \mu l v_a / d_o^2$$

From the continuity equation  $Q = v_a A_o = v_p A_p$  therefore, the braking force will be;



$$\text{where } \begin{aligned} F_b &= C_2 v_p \\ C_2 &= \frac{8 \pi \mu l}{d_p^3} (d_p/d_o)^4 \end{aligned}$$

In this way, the brake resisting force is a function of the damper piston velocity which is also the needle velocity. This makes the damper does not exert any extra damping force on the needle valve when the valve is closing and this does not change the required injection pressure of the injector. But as the needle valve opens, an extra damping force is then exerted to keep the initial rate of injection as low as possible. Due to this a high injection pressure will be developed to make the injection subsequently rises fast.

By changing the dimensions of the damper such as the piston diameter and the orifice diameter in the first damper type and the piston diameter, piston length, the throttling pipe diameter as well as the kind of the working fluid in the second type the suitable damper for each injector can be designed.

#### 4. EXPERIMENTAL STUDY

To show the effect of increasing the viscous force in the injector, it was decided to take an injector with relatively small spring stiffness (spring force) and also relatively small injection pressure forces, so the viscous force in this case can have relatively remarkable effect.

An experimental verification of the predicted results has been carried out. A schematic diagram of the experimental apparatus is shown in Fig. (5). It consists of a DC electrical-driven fuel injection pump (7) of a tangential cam type HK-10, Soviet-made. The electrically driven unit consists of an AC voltage regulator (11), a rectifier (12) and a DC electric motor (13). Also a reduction spur gear system is provided to control the number of revolutions of the injection pump cam-shaft within the range of 150-1200 rpm. The flow rate of the injected fuel can be controlled by adjusting the acting stroke of the plunger through a regulating mechanism (14). Fuel is supplied from the fuel tank (1) through the fuel valve (2), the fuel filter (3), the metering burette (4), the manual primary fuel pump (5) and the mechanical fuel feeding pump (6) to the fuel injection pump(7). The fuel is then pumped through the high pressure feeding pipeline (8) and the injector (9) to be injected inside the injection chamber (10).

The pressure transition in the delivery pipeline is recorded by using an AVL piezo quartz pressure transducer (15). The cam angle is measured every 10 degrees using a disc with 36 equally spaced grooves (16) mounted on the cam-shaft and an electric-magnetic pick-up (17). A dual beam oscilloscope (18) with a polaroid camera is used to record the pressure traces against the cam angles.

#### 5. RESULTS

To check the accuracy of the simulation method and also to find a value for the damping coefficient,  $\gamma$ , comparison between predicted and experimentally recorded results has been carried out. Different values of damping coefficient,  $\gamma$  have been tried until a reasonable agreement

between predicted and experimental results has been obtained. In this connection, it must be noted that many of the calculated functions are not recordable or its recording requires complex and expensive equipments. The parameter most easy to be recorded is the pressure.

Experimental results for the recorded pressure transition in the delivery pipeline of the injection equipment for running velocity of 500 rpm and an injection pressures of 1.5 and 2.5 MPa are shown in Fig. 6.

Figure 7 shows a comparison between the theoretical results with the corresponding experimental records of the pressure variation shown in Fig. 6, for a damping coefficient of 1.1. Although the system is difficult, one can see that there is a satisfactory agreement between predicted and experimentally recorded results.

With the simplification of the injection system simulation, it was deemed right to consider that the satisfaction agreement between the predicted and recorded results of the pressure, can be extended also to those which cannot be measured. The simulation procedure has been carried out for various values of damping coefficient  $\gamma$  higher than 1.1. Also, it was assumed that the viscous damper shown in Fig.4.b. was fitted to the injector of the considered injection system.

Predicted results of the needle lift for different damping coefficients, are shown in Fig. 8. It can be noted that the position of the beginning of the needle lift does not change with the change of the damping coefficient. This means that, insertion of the viscous damper to the injector does not change the time of the beginning of injection and the injection pressure.

Figure 8 shows also that, for the original case where  $\gamma = 1.1$ , there are two regions of primary and secondary needle lift. This result is similar to that obtained by El-Erian et al.[10]. Because the injection pressure and the spring stiffness are relatively low, the fuel pressure in the pipe reaches to the injection pressure, the needle opens and the fuel is injected. Because the pump are still pumping fuel the pressure in the fuel line at the needle reaches for a second time to the low injection pressure and the needle returns again to open and another quantity of fuel is injected. With the increase of the damping coefficient the maximum needle lift decreases in the primary region while it increases in the secondary region until  $\gamma = 3.3$  where it decreases again. The period of the first region decreases with the increase of the damping coefficient until  $\gamma = 3.3$  where it increases again. The period of the second region increases with the increase of the damping coefficient until  $\gamma = 4.4$  where it decreases again.

Prediction results of the rate of the injected fuel for different damping coefficients are shown in Fig. 9. It can be noted that every damping coefficient case has two regions of fuel injection corresponding to the two regions of the needle lift as observed in Fig.8.

From Figs. 8 and 9 it can be concluded that the fuel injection



remains until  $8^\circ$  after TDC in the original case where  $\nu=1.1$  but after that, this period increases with the increase of the damping coefficient until  $\nu = 4.4$  where it begins to decrease again but remains around the crank angle  $10^\circ$  after TDC.

Prediction results of the mass of the fuel injected as a function of the crank angle for different values of damping coefficient are shown in Fig. 10. During the period from the beginning of injection until  $3^\circ$  before TDC where the combustion is expected to start which is called the ignition delay period, it can be seen that extra damping initially keeps the rate of injection low. Then the rate of injection subsequently rises fast due to the high injection pressure development. Consequently the mass of fuel injected during the delay period does not change for damping coefficient  $\nu$  up to 2.2. As the damping coefficient increases the mass of the fuel injected during the initial period of the ignition delay period is decreased.

Fig. 11 shows the decrement percentage of the cumulative injected fuel from the original case where  $\nu = 1.1$  for different values of  $\nu$ . At the beginning of injection, the decrement percentage rises suddenly for all values of  $\nu$ . After that it takes for  $\nu = 2.2$  nearly constant value of about 30% along the ignition delay period. But for values of  $\nu$  higher than 2.2, the decrement percentage decreases and at the end of the expected ignition delay period at nearly  $3^\circ$  BTDC the decrement is ranging from 34% till 38%.

## 6. CONCLUSION

Study on the effect of the injector viscous damping on the mass of fuel injected during the delay period in diesel engines has been carried out. A numerical simulation for the fuel injection system has been developed to predict pressure transition in the different parts of the injection system, the lift of the needle valve and the rate of the injected fuel. The finite difference principle has been incorporated in the used simulation method. The injector is considered to be provided with a suitable damping unit to increase the viscous friction force which resist the needle valve lift and the influence of the damping unit on the injection process has been examined theoretically.

The obtained results show that an extra damping keeps the rate of fuel injection low at the start of injection, then due to the high pressure developed the rate of injection is subsequently rises rapidly. The insertion of the viscous damper to the injector does not make any change in the time of the beginning of injection and the injection pressure. By increasing the damping coefficient a reduction of the amount of injected fuel during the delay period has been obtained. A percentage decrement ranging from 30 to about 38% of the injected fuel during the expected delay period has been predicted for damping coefficients of 2.2, 3.3, 4.4, 5.5 and 11.

To determine what actually happens to the delay period when extra damping is added, it is recommended that experiments have to be carried out on an engine fitted with a hydraulic damper. Also the effect of the damping coefficient on the mass of fuel injected during the delay period can be investigated for any combination of speed and load.

## 7. NOMENCLATURE

a	Cross sectional area of pipe
$a_v$	Area of valve exposed to pressure
A	Equivalent flow area of two orifices in series
A	Maximum valve cross sectional area
$A_1$	Flow area at the needle seat
$A_2$	The total flow area through the injection holes
$A_d$	Valve differential area
$A_p$	Total area of plunger
$B_0, \dots, B_3$	Constants
C	Constant
$C_d$	Coefficient of discharge
d	Diameter of sac volume
f	Coefficient of viscous friction (Damping coefficient)
G	Rate of fuel increase with time
K	Bulk modulus of fuel or spring stiffness
L	Needle lift
M	Mass of moving parts (needle valve and lift pick up)
P	Instantaneous pressure at the point under consideration
$P_f$	Instantaneous sum of the forward pressure waves
$P_r$	Instantaneous sum of the backward pressure waves
$P_k$	Residual pressure in the pipe injection
$P_1$	Injection pressure
$P_2$	Cylinder pressure
Q	Rate of discharge
$Q_{inj}$	Rate of fuel injection
$Q_l$	Rate of leakage
$S_1, S_2$	Constants
t	Time
v	Velocity of fuel in the pipe at point consider
$v_p$	Velocity of pump plunger
$V_n$	Volume of fuel concentrated at nozzle end
$V_p$	Volume of fuel concentrated at pump end
x	Needle displacement
$\dot{x}$	Needle velocity
$\ddot{x}$	Needle acceleration
$\rho$	Fuel density
$\nu$	Damping coefficient
$\omega_n$	Natural frequency

## 8. REFERENCES

1. Austen, A. E. W. and Priede, T., *Origines of Diesel Engine Noise*, Proc. Symp. on Engine Noise and Noise Suppression, I. Mech. E., London, (1958), pp. 19-32.
2. Russell, M. F. and Haworth, R., *Combustion Noise from High Speed Direct Injection Diesel engines*, SAE paper No. 850973, (1985), pp. 4.810-4.831.
3. Kau, C. J., Heap, M. P., Tyson, T. J. and Wilson, R. P., *The Prediction of Nitric Oxide Formation in a Direct Injection Diesel Engine*, Proc. 16th Symp. on Comb. (Int.), The Combustion Inst., Pittsburgh, (1977), pp. 337-350.



4. Griffen, E. and Rowe, A.W., Pressure Calculation for Oil Engine Fuel Injection Systems, I. Mech. Eng. Proc., Vol 141, (1939)
5. Knight, B. E., Fuel Injection System Calculation, I. Mech. Eng. Proc. Auto Div., No. 1, (1960-1961), p. 25.
6. Becchi, G.A., Analytical Simulation of Fuel Injection in Diesel Engines, SAE Paper No. 710568, (1971), pp. 1825-1854.
7. Rosselli, A. and Badgley, P., Simulation of the Cummins Diesel Injection System, SAE Paper No. 710570, (1971), pp. 1870-1880.
8. Wylie, E.B., Bolt, J.A. and El-Erian, M. F., Diesel Fuel Injection System Simulation and Experimental Correlation, SAE Paper No. 710569, (1971), pp. 1855-1869.
9. El-Erian, M.F., Wylie, E. B. and Bolt, J. A., Analysis and Control of Transient Flow in the Diesel Injection System, Part I, The Analytical Control Method, SAE Paper No. 730661, (1973), pp. 2318-2334.
10. El-Erian, M.F., Wylie, E. B. and Bolt, J. A., Analysis and Control of Transient Flow in the Diesel Injection System, Part II, Design Results of Controlled After Injection, SAE Paper No. 730662, (1973), pp. 2335-2446.
11. Yamaoka, K. and Saito, S., Computer Technique for Evaluation of Cavitation Characteristics of Certain Phases of Fuel Injection System, SAE Paper No. 730663, (1973), pp. 2347-2363.
12. Yamaoka, K., Saito, S., Nobuyuki, A. and Okazaki, M., Analysis of Bypass Control Fuel Injection System for Small Diesel Engines by Digital Computer, SAE Paper No. 730664, (1973), pp. 2364-2395.
13. Matsuoka, S., Yokota, K., Kamimoto, T. and Igoshi, M., A Study of Fuel Injection Systems in Diesel Engines, SAE Paper No. 760551, (1976), pp 1854-1872.
14. Dennis, H. G., A Flexible Fuel Injection Simulation, SAE Paper No. 861567, (1986), pp 6896-6906.
15. Will, D. and Stroehl, H., Einfuehrung in die Hydraulik und Penumatik, VEB Verlag Technik Berlin, 1983.

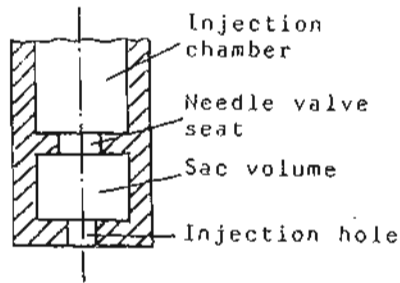


Fig. 1 The lower part of an injector nozzle.

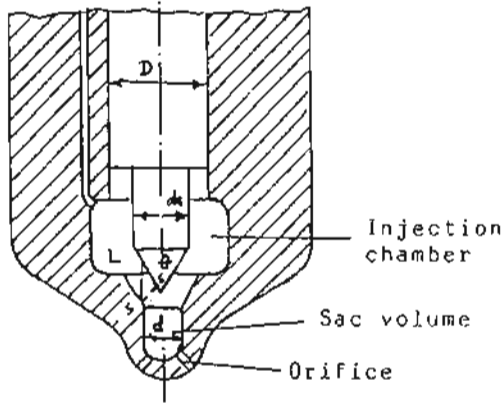


Fig. 2 Section through the lower part of the nozzle.

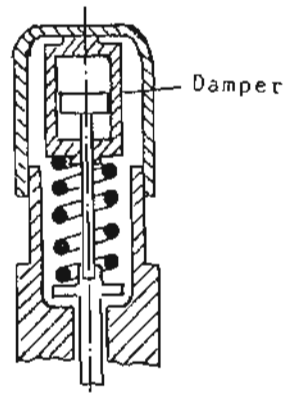


Fig. 3 The damper fitted to the injector.

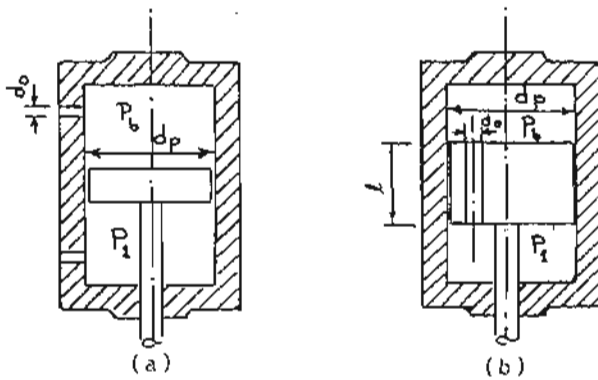


Fig. 4 The viscous dampers.

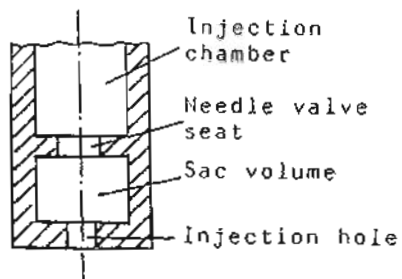


Fig. 1 The lower part of an injector nozzle.

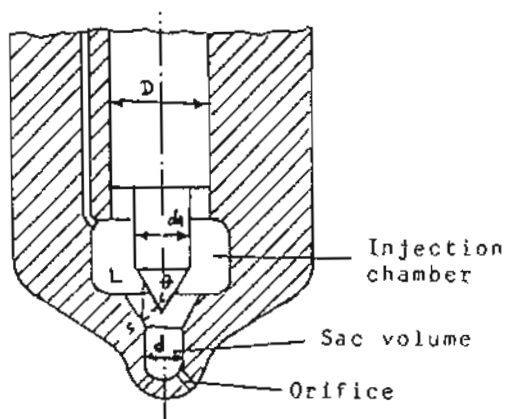


Fig. 2 Section through the lower part of the nozzle.

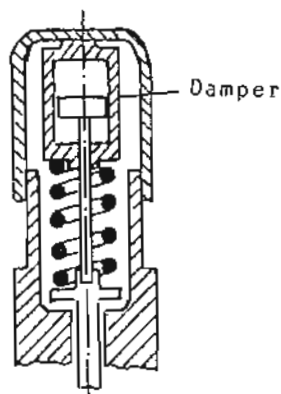


Fig. 3 The damper fitted to the injector.

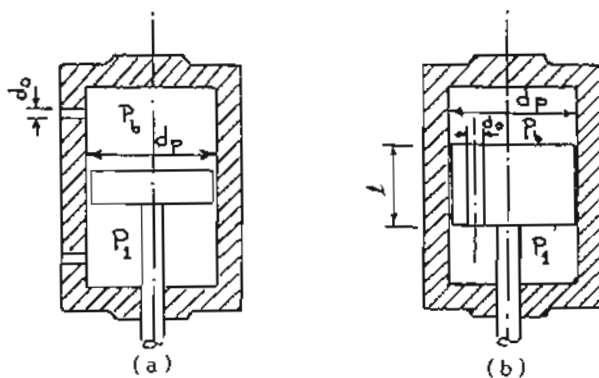


Fig. 4 The viscous dampers.

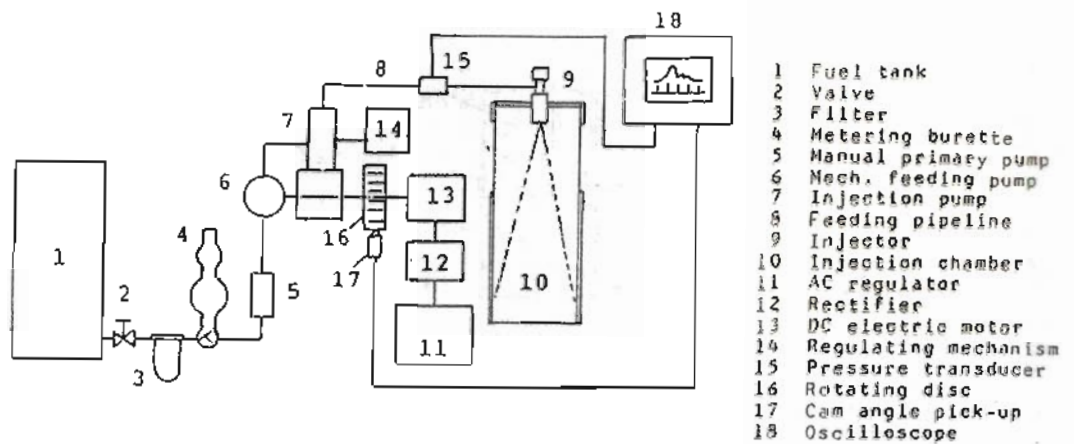
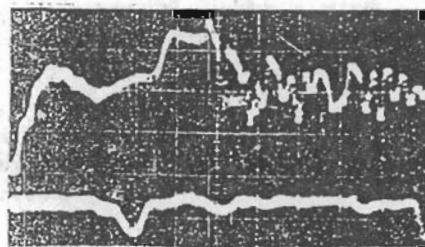
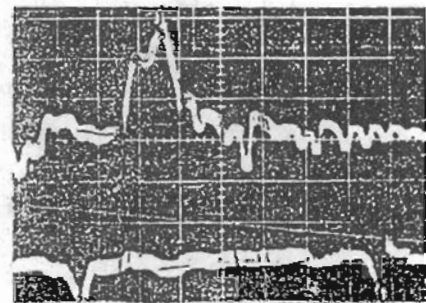


Fig. 5 Schematic diagram of the experimental setup.



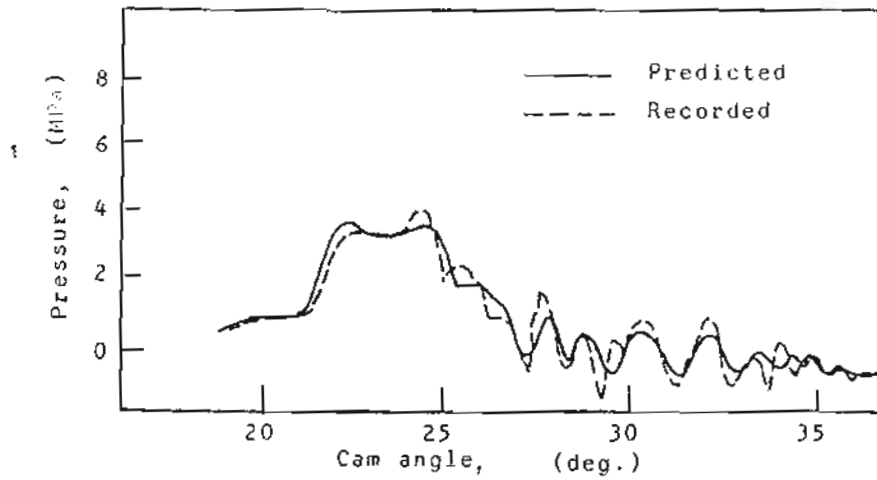
(a)  $P_i = 1.5$  MPa



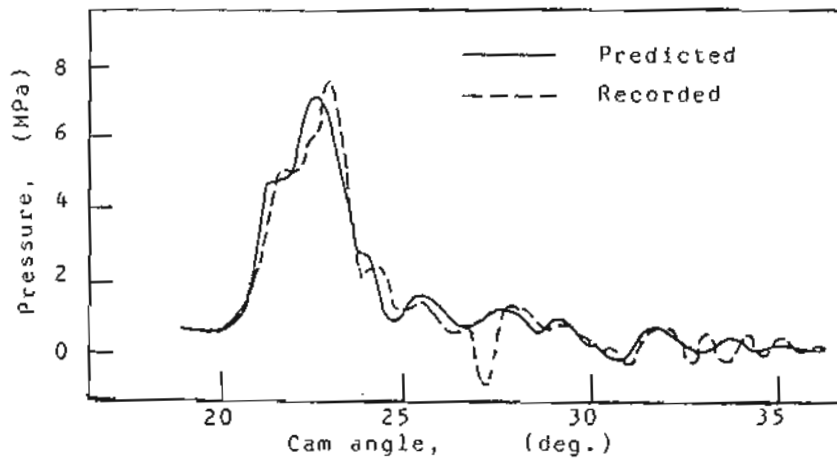
(b)  $P_i = 2.5$  MPa

Fig. 6 Recorded pressure variation at the half of the delivery duct of the injection system.



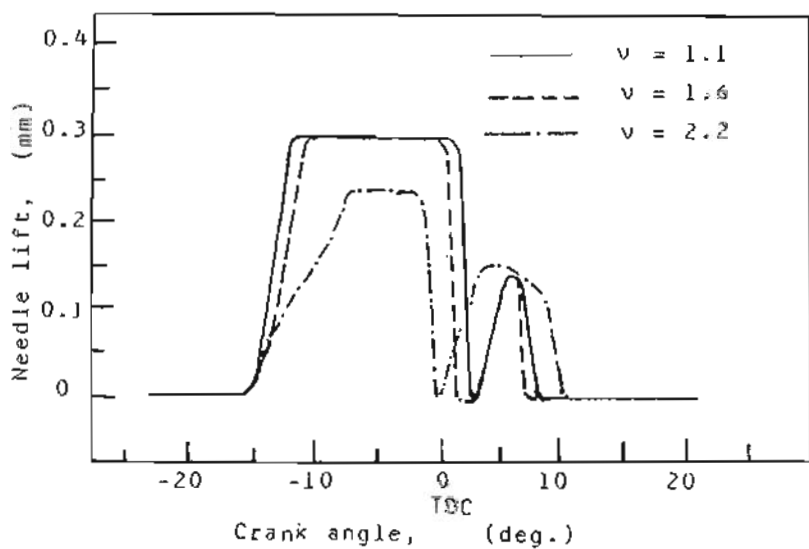


(a)  $P_i = 1.5$  MPa

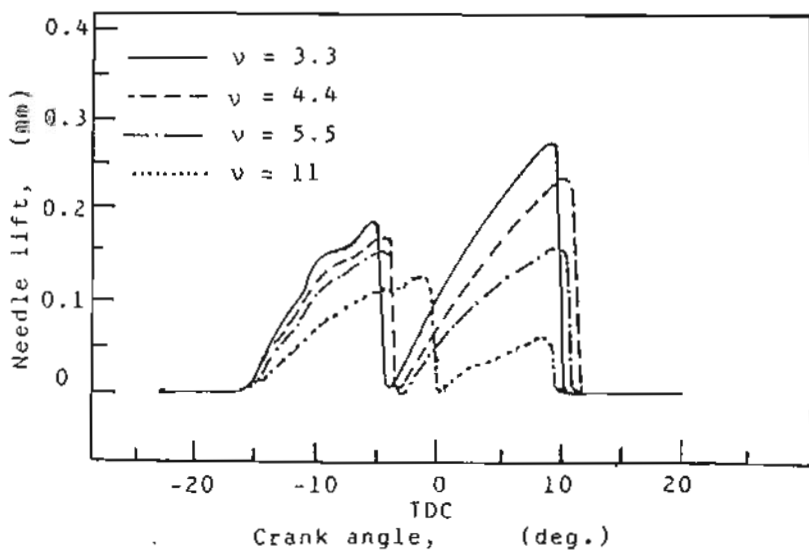


(b)  $P_i = 2.5$  MPa

Fig. 7 Pressure variation at the half of the delivery duct of the injection system at two different injection pressures.

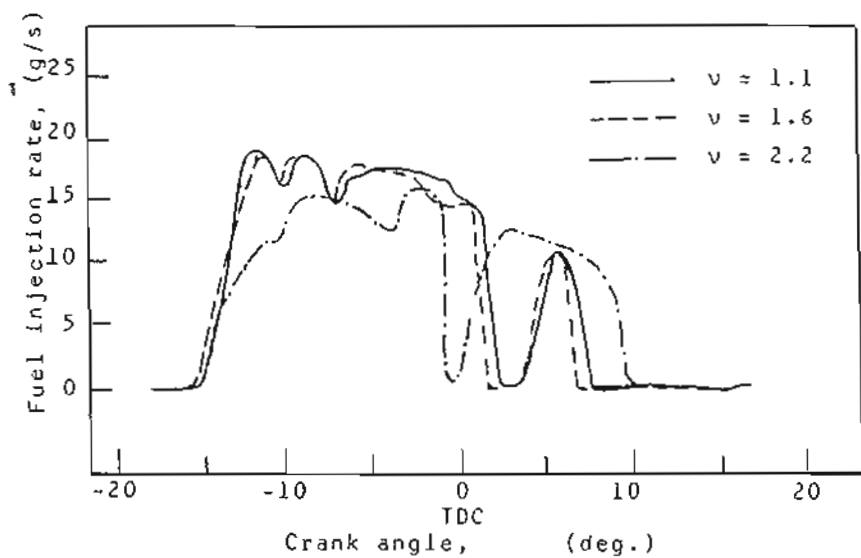


(a) For damping coefficients,  $\nu = 1.1, 1.6$  &  $2.2$

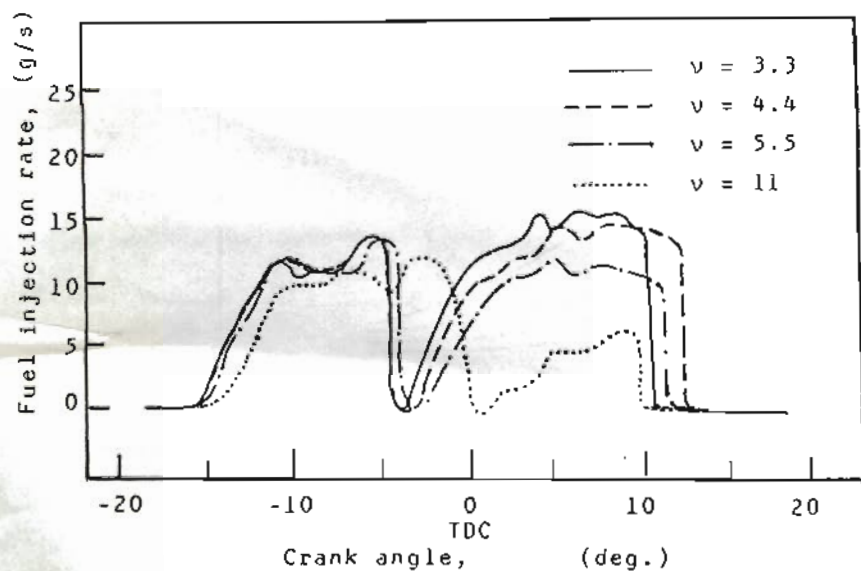


(b) For damping coefficients,  $\nu = 3.3, 4.4, 5.5$  &  $11$

Fig. 8 Predicted needle lift for different damping coefficients.



(a) For damping coefficients,  $\nu = 1.1, 1.6 \text{ \& } 2.2$



(b) For damping coefficients,  $\nu = 3.3, 4.4, 5.5 \text{ \& } 11$

Fig. 9 Fuel injection flow rate with different gamping coefficients.

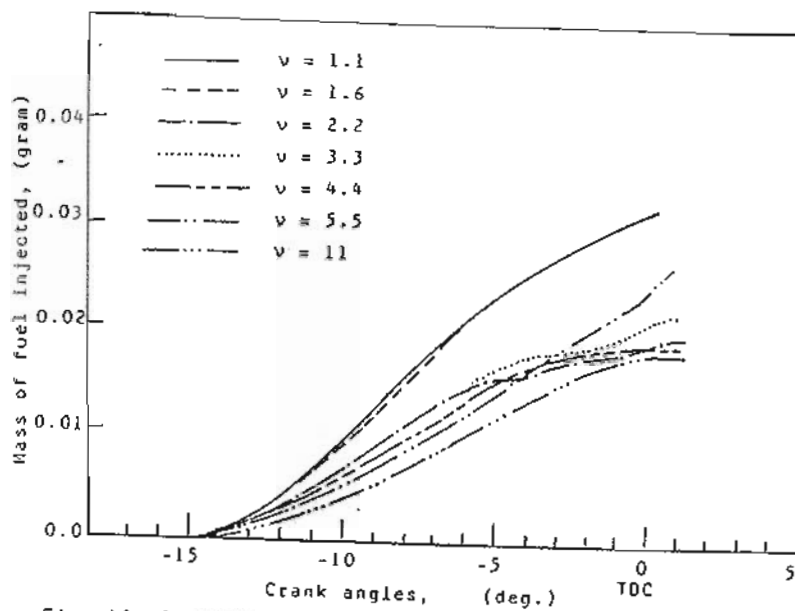


Fig. 10 Cumulative mass of fuel injected with different damping coefficients.

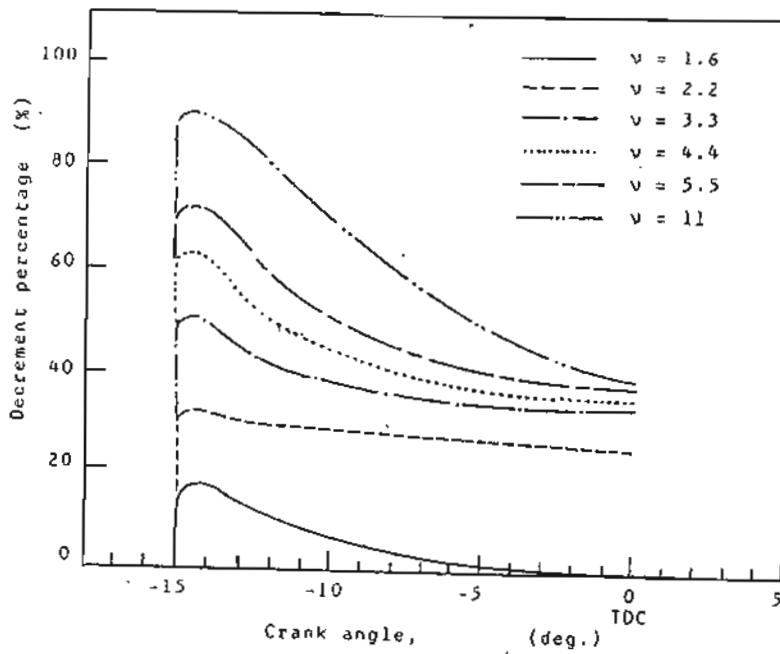


Fig. 11 Decrement percentage of cumulative mass of the injected fuel with different damping coefficients.